ОБЪЕДИНЕННЫЙ
ИНСТИТУТ
ЯДЕРНЫХ
ИССЛЕДОВАНИЙ

Дубна

E15-95-475

S.A.Karamian, J. de Boer[1], Yu.Ts.Oganessian, A.G.Belov,
Z.Szeglowski, B.N.Markov, I.Adam, V.I.Stegailov,
Ch.Briancon[2], O.Constantinescu[3], M.Hussonnois[3]

OBSERVATION OF PHOTONUCLEAR REACTIONS ON ISOMERIC TARGETS: $^{178}Hf^{m_2}(\gamma, n)^{177}Hf^{m_2}$, $^{180}Ta^{m}(\gamma, 2n)^{178}Ta^{m,g}$ AND $^{180}Ta^{m}(\gamma, p)^{179}Hf^{m_2}$

Submitted to «Zeitschrift für Physik A»

[1]Ludwig-Maximilians-Universität München, D-85748 Garching, Germany
[2]CSNSM, 91405, Orsay, France
[3]IPN, 91406 Orsay, France

1995

1 Introduction

Nuclear reactions with high-spin isomers are of interest for the investigation of nuclear structure effects. Special features are expected in the reaction cross-sections and angular distributions. Furthermore, high-spin levels may be excited with higher probability. Of special interest is the question of structure selectivity for the population of levels in the residual nucleus. This selectivity is well known for excited levels below ~3 MeV populated in β- and γ-decays. It is important to know whether an initial structure of the target nucleus influences the feeding intensities of the levels in the reaction product or if it is governed just by spin and excitation energy, in accordance with the statistical-model predictions.

Photonuclear reactions starting from a high-spin isomer can be important for the study of giant resonances built on quasiparticle states as well as for the study of the amount of K-mixing at high excitations energies. The interest in such reactions may also be motivated by the possible applications, e.g. the search for efficient ways of γ-laser pumping.

Some years ago the strong depopulation of the $^{180}Ta^{m}$ isomeric state (m) by the (γ,γ')-reaction was investigated [1]. After more detailed studies [2] the idea of strong K-mixing was introduced for the levels at an excitation energy $E^{*} \geq 2.8$ MeV which serve as intermediate states z for the $m \rightarrow z \rightarrow g$ (ground state) transitions. In Coulomb excitation the depopulation of $^{180}Ta^{m}$ was observed [3], however the measurements were disturbed by possible transfer reactions on ^{181}Ta.

Another program focuses on the study of the $^{178}Hf^{m_2}$ isomer, both with regard to aspects of nuclear structure and of nuclear-reaction mechanisms. This isomer is a four-quasiparticle, 16^{+}, long-lived (31 years) yrast trap. It can be considered as a unique object for reaction studies. The methods for production, chemical and mass-separation of the $^{178}Hf^{m_2}$ isomer were developed [4] and resulted in the production of as many as $2 \cdot 10^{15}$ atoms until now. Several nuclear reactions such as Coulomb excitation, (d,d'), (p,t) and (n,γ)-reactions using a $^{178}Hf^{m_2}$ target were successfully investigated. One can find the results in the original papers [5-7] and review talks [8-10]. Many problems are under continuous investigation and among them the problem of the levels population in products of nuclear reactions with exotic isomeric targets.

Let us assume that the reaction starts from an isomeric state and finally populates both isomeric and ground states in a residual nucleus. The measured ratio of the isomeric-to-ground state yields can throw some light on the feeding selectivity especially if the initial and final isomeric states have similar single-particle structure.

The yields of the exotic reactions: $^{178}Hf^{m_2}(\gamma,n)^{177}Hf^{m_2}$, $^{180}Ta^{m}(\gamma,2n)^{178}Ta^{m,g}$ and $^{180}Ta^{m}(\gamma,p)^{179}Hf^{m_2}$, as well as yields of many other photonuclear reactions on ground states of Ta and Hf nuclei were measured by the method of the γ-spectroscopy off-line after the targets activation by the bremsstrahlung radiation. The properties of the isomeric and ground states of the involved nuclei are presented in fig. 1. Their decay γ-lines are listed in table 1.

2 The $^{178}Hf^{m_2}(\gamma,n)^{177}Hf^{m_2}$ reaction

The single-particle structures of the target and product nuclei are attributed to the ($\pi 7/2^{+}$, $\pi 9/2^{-}$, $\nu 7/2^{-}$, $\nu 9/2^{+}$) and ($\pi 7/2^{+}$, $\pi 9/2^{-}$, $\nu 5/2^{-}$, $\nu 7/2^{-}$, $\nu 9/2^{+}$) configurations, respec-

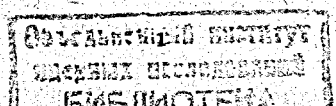

tively. Only one neutron-pair has to be decoupled in the reaction. Also the spin difference between initial and final channels of the reaction (-3/2 $\hbar$) is low enough to expect a relatively high yield for the production of the $^{177}Hf^{m_2}$ five-quasiparticle, $K^\pi = 37/2^-$ isomer in the (γ,n)-reaction on the four-quasiparticle, $K^\pi = 16^+$ $^{178}Hf^{m_2}$ isomeric target.

The experimental scheme is rather simple: a $^{178}Hf^{m_2}$ sample is irradiated by the bremsstrahlung, and the induced γ-activity is thereafter measured by a Ge-detector to search for the γ-lines decaying from the 51.4 min $^{177}Hf^{m_2}$ isomer. However, due to the low level of activity the difficulties arise.

To increase the detector efficiency the sample must be placed so close to the detector that the Compton suppression is ineffective because the anti-Compton scintillator will be fired by almost each γ-cascade of high-multiplicity. As seen in table 1 most intense γ-lines of $^{177}Hf^{m_2}$ are lower in energy than the $^{178}Hf^{m_2}$ lines, so the Compton spectrum of the $^{178}Hf^{m_2}$ isomer gives rise to large background in the region of the $^{177}Hf^{m_2}$ lines. Only one line, 638.2 keV, lies in an energy region which is free from the $^{178}Hf^{m_2}$ Compton spectrum, and it was therefore chosen as a reference.

In the measurements it was seen immediately that the $^{178}Hf^{m_2}$ source generates high counting rates at energies above the most energetic line, 574.2 keV, because of the addition of the γ-cascade quanta in the close geometry which was is used. The spectrum around 630 keV is shown in fig. 2a. One can see four sum peaks in this portion of the spectrum with a strong one at 639.8 keV, obscuring the 638.2 keV line of $^{177}Hf^{m_2}$. Basing on the E_γ values listed in table 1 for $^{178}Hf^{m_2}$ one can evaluate as many as 150 sum-energy lines of different intensity. The majority of them were seen in the measured spectra. To suppress the relative intensity of the sum peaks in the spectrum the source-detector distance could be increased, however, this leads to an unacceptable loss in efficiency.

Some of the sum lines can be suppressed using absorbers. The 639.8 keV line, for instance, is formed by summing the energies of 213.4 keV and 426.4 keV transitions. When the line of 213.4 keV is absorbed in 7 mm Pb the satellite line is suppressed by two orders of magnitude as it is seen by the comparison of figs 2a and 2b spectra. The remaining background is due to the adding of Compton-effect signals in the detector. The introduction of the absorber reduces the detection efficiency for the 638.2 keV γ-quanta by a factor of two both due to an absorption and a source-detector distance increase. However, the background suppression is much more significant.

Another important source of background is the bremsstrahlung-induced activation of the material used as a backing and as a catcher. Of many tested materials beryllium was found to be the best since it is activated only weakly by the bremsstrahlung. A problem is posed by the activation of contaminant elements present in Be such as Cl, Sc, Ti, Cr, Fe, Ni, Zn, Cu, Ga, Sr, Zr. A high-purity 20 μ Be foil was finally used producing near 630 keV a smooth Compton spectrum with an intensity below that of the spectrum generated by the $^{178}Hf^{m_2}$ self-activity.

The $^{178}Hf^{m_2}$ material was purified using a special chemical procedure (ref. [11]). Efforts were made to avoid any ballast activity and weight admixtures in the $^{178}Hf^{m_2}$ material. Finally $^{178}Hf^{m_2}$ target layer was chemically deposited onto the Be substrate, dried and heated up to reach the oxide form. Two of the $^{178}Hf^{m_2}$ targets with the Be catcher foil between them were coupled closely and this stack was exposed to a bremsstrahlung radiation.

The catcher collects $^{177}Hf^{m_2}$ atoms recoiling from the targets due to neutron emission in the (γ, n)-process. A total of $0.9 \cdot 10^{14}$ atoms of $^{178}Hf^{m_2}$ on the two targets were exposed.

The catcher is needed to minimize the activity of the sample measured. The $^{178}Hf^{m_2}$ activity is transferred to the catcher only as a contaminant because of the direct contact with the $^{178}Hf^{m_2}$ layers under exposure. The use of a cather leads to some loss of $^{177}Hf^{m_2}$ activity, but it eliminates the bulk of the $^{178}Hf^{m_2}$ activity. So the effect-to-background ratio is improved by the use of the catcher.

Since a collection efficiency, ε_c, of the catcher influences the final result, it was calculated using the ranges (measured in ref.[12]) of the ^{196}Au recoils formed in the ^{197}Au (γ, n) reaction at E_e=24.2 MeV. The average range was found [12] to be about 5.0 $\mu g/cm^2$ in Au, this figure was corrected for the case of the ^{177}Hf recoils in the HfO_2 matter. The thickness of the 8mm in diameter target-layer was estimated to be 3.5$\mu g/cm^2$ of the HfO_2. The estimation is based on the measured $^{178}Hf^{m_2}$ activity and the known [4] ratio of the $^{178}Hf^{m_2}$ to the total Hf yields in the producer reaction. The presence of any contaminants was neglected.

The average ε_c value was calculated taking into account the range dispersion due to the neutron energy spectrum, the angular dependence of the range [12] and natural range straggling. Some indefinity in the chemical form of the Hf material and possible inhomogenity of the layer thickness force us to increase the effective target thickness by a factor of 1.4. This more or less arbitrary factor has to be introduced in the result error. Finally, the efficiency was found to be about $\bar{\varepsilon}_c$=0.24 of 4π.

A series of irradiations were carried out to measure the $^{177}Hf^{m_2}$ yield in the (γ,n)-reaction. A 15 μA 24 MeV electron beam from the Dubna MT-25 microtron was impinging on a 2.5 mm W converter (fig. 3). The stack of the samples was placed just behind the W converter. A Ta foil was used as a calibration target.

After a 2 h exposure of the stack using the maximum intensity of the microtron beam the γ-spectrum of the catcher was measured during 2 h by a high-resolution "Canberra" HP Ge-detector in close geometry with a 7 mm Pb + Cd + Cu absorber. The detector was placed into a lead housing to suppress the background from natural radioactivity. Exposures and measurements were repeated 8 times under the same conditions and the accumulated spectra were added.

From the accumulated spectrum the following background spectra were subtracted:

1. A detector background proportional to the measurement time.
2. The spectrum due to the $^{178}Hf^{m_2}$ activity.
3. The spectrum of the ^{nat}Hf activation by the bremsstrahlung proportional to the ^{nat}Hf quantity in the sample, the collection efficiency and the integrated irradiation intensity.
4. The spectrum of the catcher's material activation.

Each background spectrum was measured separately with sufficient statistics in order to minimize the inaccuracy of the final result.

The resulting spectrum is shown in fig. 4a. The peak at the right energy position, 638.2 keV, has an area of about 70 $\pm$ 26 counts. It is attributed to $^{177}Hf^{m_2}$ produced in the $^{178}Hf^{m_2}$ (γ,n) reaction. The decay observed for this tiny peak is consistent with the known 51.4 min half-life of $^{177}Hf^{m_2}$. The more intense peak at 634 keV is attributed to ^{74}As produced in the (γ, n) reaction on an As contamination in the isomeric Hf material.

From the area of the 638.2 keV peak we could deduce the number of $^{177}Hf^{m_2}$ atoms produced during the irradiation. All the necessary efficiency and time factors were taken into account. After that the photonuclear reaction yield was evaluated as:

$Y = \frac{N_{at}^{pr}}{N_{at}^{tar} N_e}$,

where N_{at}^{pr} is the number of atoms produced, N_{at}^{tar} is the number of target atoms and N_e is the integral number of electrons hitting the converter during the irradiation. The yield defined in such a way includes the conversion efficiency, the shape of the bremsstrahlung spectrum and geometry factors. However, the ratio of yields is physically significant since it is defined by the integrated cross-section ratios for the production of any final states.

The measured $^{177}Hf^{m_2}$ yield is accurate within a factor of 2 mainly due to the statistical error in the peak area and uncertainties in the calculated collection efficiency. The ground state of the ^{177}Hf being stable cannot be detected by the activation technique. So, the yield Y ($^{177}Hf^{m_2}$) can be compared to the $^{181}Ta(\gamma,n)\,^{180}Ta^g$ reaction yield measured for calibration under identical conditions and the ratio was found to be

$\frac{Y(^{177}Hf^{m_2})}{Y(^{180}Ta^g)} = 0.12\pm^{0.05}_{0.04}$.

The properties of the calibration reaction are not expected to be very different from the studied one: the thresholds of both reactions are nearly the same as well as the widths and positions of giant resonances. Therefore the yield ratio reflects the isomer-to-ground state ratio for the $^{178}Hf^{m_2}(\gamma,n)\,^{177}Hf^{m_2,g}$ reaction. It means that the ground state is populated with a large probability and only about 12% of the reaction events lead to the $37/2^-$, m_2 isomeric state in ^{177}Hf.

3 $^{180}Ta^m(\gamma,2n)^{178}Ta^{m,g}$ and $^{180}Ta^m(\gamma,p)^{179}Hf^{m_2}$ reactions

The reactions with $^{180}Ta^m$ (9^-) isomer were studied using natural (^{nat}Ta) targets despite the very low abundance ($1.2\cdot10^{-2}$%) of this nuclide. The irradiation scheme was similar to that shown in fig. 3.

For the observation of the $(\gamma,2n)$-reaction a 10μ Ta foil was exposed to the bremsstrahlung and its γ-activity was measured by a Ge detector after irradiation. In the series of irradiations time intervals of the exposures and measurements were optimized taking into account the lifetimes of the detected activities: $^{178}Ta^m$ - 2.4 h and $^{178}Ta^g$ - 9.3 min. It is so far unknown what state is the isomer and what is the ground state in ^{178}Ta. Hereafter we shall call the high-spin (7^-, 2.4h) state as isomeric and the (1^+, 9.3 min) as the ground state. This arbitrary nomination is introduced just for the simplicity of the discussion.

The major γ-lines (see table 1) of $^{178}Ta^m$ and $^{178}Ta^g$ were observed in the γ-spectra with good statistics, as described in the preliminary publication [13]. For example, one spectrum of the ^{nat}Ta sample activated by a 22 MeV bremsstrahlung radiation taken after 1h cooling is shown in fig.4b, the γ-lines of the ^{178}Ta^m are evident. More intense lines of $^{180}Hf^m$ are seen too.

The abundant reaction $^{181}Ta(\gamma,n)^{180}Ta^g$ (8.15h) was used for the yield calibration. This reaction does not create a large background in the detector since the $^{180}Ta^g$ nucleus emits in the decay only Hf, W K-X rays and soft γ-lines (93.3 and 103.6 keV) which are easily suppressed by a 1 mm Pb absorber.

Both activities of ^{178}Ta, 9.3 min and 2.4 h, could be measured from 17 up to 24 MeV end-point energy (E_e) of the bremsstrahlung spectrum. Independently of E_e the isomer-to-

Table 1. Major γ-lines of the $^{177}Hf^{m_2}$, $^{178}Hf^{m_2}$, $^{179}Hf^{m_2}$, $^{178}Ta^m$, $^{178}Ta^g$, $^{180}Ta^g$, $^{177}Lu^g$, $^{178}Lu^m$, $^{178}Lu^g$ (as compiled in Nucl. Data Sheets)

$^{177}Hf^{m_2}$		$^{178}Hf^{m_2}$		$^{179}Hf^{m_2}$		$^{178}Ta^m$		$^{178}Ta^g$		$^{180}Ta^g$	
E_γ,keV	I_γ,%	E_γ,keV	I_γ,%	E_γ,keV	I_γ,%	E_γ,keV	I_γ,%	E_γ,keV	I_γ,%	E_γ,keV	I_γ,%
113.0	27.0	88.9	62.0	122.7	28.0	88.9	64.3	93.2	6.7	Hf Kα	57
128.5	20.2	93.2	17.3	146.1	27.3	93.2	17.2	1106.1	0.53	Hf Kβ	15
153.3	21.8	213.4	80.9	169.8	19.6	213.4	81.4	1183.5	0.17	W Kα	0.46
208.4	73.0	216.7	63.7	192.8	21.8	216.7	0.24	1340.9	1.02	W Kβ	0.12
214.0	40.9	237.4	8.8	217.0	9.1	325.6	94.1	1350.6	1.17	93.3	4.34
228.5	48.0	257.6	16.6	236.6	19.0	331.6	31.2	1402.9	0.48	103.6	0.78
277.3	75.8	277.4	1.5	268.9	11.4	426.4	96.9	1496.1	0.27		
295.1	69.0	296.8	9.8	316.0	20.5	$^{177}Lu^g$		$^{178}Lu^m$		$^{178}Lu^g$	
311.5	58.8	325.6	93.9	362.6	40.1	71.7	0.15	88.5	63.1	93.2	6.24
326.7	65.4	426.4	96.9	409.8	21.7	112.9	6.4	93.2	17.2	203.8	0.32
327.7	23.7	454.0	16.3	453.7	68.6	208.4	11.0	213.5	81.4	1269.2	0.97
378.5	39.3	495.0	68.7			249.7	0.21	325.3	94.1	1309.9	1.46
418.5	28.1	535.0	8.9			321.3	0.22	331.5	13.2	1340.8	4.59
638.2	20.1	574.2	83.6					426.2	96.9	1496.0	0.33

Table 2. Bremsstrahlung-induced reaction yields measured at E_e = 23.5 MeV with ^{nat}Ta, ^{nat}Hf and $^{178}Hf^{m_2}$ targets

Reaction	J_t	J_g	J_m	$Y, 10^{-26}$ *)	Y_m/Y_g **)
$^{181}Ta(\gamma,n)^{180}Ta^g$	7/2	1	9	6.2	–
$^{181}Ta(\gamma,p)^{180}Hf^m$	7/2	0	8	3.5 10^{-4}	0.04
$^{181}Ta(\gamma,\alpha)^{177}Lu^g$	7/2	7/2	23/2	4.2 10^{-5}	–
$^{180}Ta^m(\gamma,2n)^{178}Ta^m$	9	1	7	0.39	3.0
$^{180}Ta^m(\gamma,2n)^{178}Ta^g$				0.13	
$^{180}Ta^m(\gamma,p)^{179}Hf^{m_2}$	9	9/2	25/2	0.8 10^{-3}	0.09
$^{180}Hf(\gamma,\gamma')^{180}Hf^m$	0	0	8	4.9 10^{-4}	0.0029
$^{180}Hf(\gamma,p)^{179}Lu$	0	7/2	–	0.97 10^{-2}	–
$^{179}Hf(\gamma,\gamma')^{179}Hf^{m_2}$	9/2	9/2	25/2	2.4 10^{-4}	0.0014
$^{179}Hf(\gamma,p)^{178}Lu^m$	9/2	1	9	2.4 10^{-3}	0.75
$^{179}Hf(\gamma,p)^{178}Lu^g$				3.2 10^{-3}	
$^{178}Hf(\gamma,p)^{177}Lu^m$	0	7/2	23/2	$\leq$5 10^{-5}	$\leq$ 0.005
$^{178}Hf(\gamma,p)^{177}Lu^g$				1.1 10^{-2}	
$^{178}Hf^{m_2}(\gamma,n)^{177}Hf^{m_2}$	16	7/2	37/2	0.7	0.12
$^{177}Hf(\gamma,2n)^{175}Hf$	7/2	5/2	–	7.5	–
$^{176}Hf(\gamma,n)^{175}Hf$	0	5/2	–		
$^{174}Hf(\gamma,n)^{173}Hf$	0	1/2	–	5.9	–
$^{174}Hf(\gamma,2n)^{172}Hf$	0	0	–	0.34	–

*) For the yield definition see text.

**) Random errors of the Y_m/Y_g values are typically about $\pm$ (15-20)%, and the systematical ones are discussed in the text.

ground state ratio was found to be:

$Y_m/Y_g = 3.0 \pm 0.4$

for the reaction $^{180}Ta^m(\gamma,2n)^{178}Ta^{m,g}$. The 2.4 h lived, 7^- state is populated in 75% of the events and the 1^+ state with a probability of 25%.

The background reaction on the abundant isotope $^{181}Ta(\gamma,3n)$ has a threshold of 22.1 MeV. Thus it cannot contribute to the ^{178}Ta yield as long as the bremsstrahlung end-point energy is kept below 22 MeV.

The total reaction yield of the $^{178}Ta^m + {}^{178}Ta^g$ turns out to be 1.5 $\pm$0.2 times higher than the yield of the $(\gamma,2n)$ reaction on a zero-spin target nucleus, determined by the yield measurement for the $^{174}Hf(\gamma,2n)^{172}Hf$ reaction. This excess factor (1.5) could be a manifestation of the special properties of a high-spin target; perhaps the giant-resonance parameters are different from the standard ones.

The $^{180}Ta^m(\gamma,p)^{179}Hf^{m_2}$ reaction produces much lower activity than the $(\gamma,2n)$ reaction, so the 1 g sample of ^{nat}Ta was exposed at E_e = 23.5 MeV during 20 hours. The contribution of the $^{181}Ta(\gamma,d)^{179}Hf^{m_2}$ reaction is negligible. The yield of the 25.1 d $^{179}Hf^{m_2}$ was measured by looking for the most intense lines, 362.6 and 453.7 keV, in the presence of radiation of the $^{182}Ta(115d)$ produced in the (n,γ) reaction by the neutron flux created in the converter by the e-beam. The lines at 364.2 and 451.4 keV are identified as sum peaks of ^{182}Ta decay γ-lines. Gamma lines of activated impurities (Fe, Nb, Zr...) are also present in the spectra. After a 100 h measurement one can distinguish in the spectrum tiny peaks belonging to $^{179}Hf^{m_2}$, see in fig.4c. The yield was evaluated from the intensity of these lines. In order to estimate the isomer-to-ground state ratio this yield was compared to the usual (γ,p)-reaction yield. The last one was determined in a separate experiment where a ^{nat}Hf target was exposed and the lutecium isotopes ^{177}Lu and ^{179}Lu were detected. This yield was multiplied by a factor of 1.5 for the account of the yield enhancement revealed in the $^{180}Ta^m(\gamma,2n)$ reaction.

The Y_m/Y_g ratio for the $^{180}Ta^m(\gamma,p)^{179}Hf$ reaction at E_e = 23.5 MeV was determined to be:

$\frac{Y_m}{Y_g} = 0.09 \pm 0.03$.

The isomer-to-ground state ratios have thus been determined for three reactions on isomeric targets. An accuracy is limited by some restriction in experimental conditions. So the studies should be continued since the photoabsorption cross-section for high-spin quasiparticle states has never been studied in detail, neither theoretically nor experimentally. More precise experiments than described here require highly enriched targets which are not available today.

4 Systematics of the Y_m/Y_g values and discussion

It was already mentioned that many reactions on the ground state nuclei of Hf and Ta were studied for the calibration and comparison with the results taken on isomeric targets. The yield values are presented in Table 2 for a 23.5 MeV bremsstrahlung end-point energy. The results deviate in some detail from those in the review [14]; for instance, in the ^{nat}Hf irradiations we cannot detect $^{177}Lu^m$, but $^{179}Hf^{m_2}$, ^{179}Lu, $^{178}Lu^{m,g}$ and $^{177}Lu^g$ are observed sucessfully. (Their γ-lines see in table 1).

$^{179}Hf^{m_2}$ and $^{180}Hf^m$ were produced in the (γ,γ') reactions. The total yield of the (γ,γ') products was evaluated from the (γ,n)-yield taking into account the GDR parameters, the

shape of the bremsstrahlung spectrum and the measured excitation function of the (γ,γ') processes [15]. Thus Y_m/Y_g values were found to be on the level of 2.10^{-3} for the cases when $^{180}Hf^m$ and $^{179}Hf^{m_2}$ isomers were excited in a photon inelastic scattering.

The results of our measurements together with the literature data could be sufficient to construct a semiempirical systematics of Y_m/Y_g values in photon induced reactions. Let us motivate the neccessity of such systematics. Being plotted it allows us to check whether a special nuclear structure of an isomeric state (used as a target) plays an important role in the population of high-spin isomer in the reaction product. In other words some light on the selectivity of the level population in the deexcitation cascades can be thrown. In particular, the role of K-quantum number at high excitation energies can be clarified.

One can suggest that the best way of such evaluation is the comparison of the experimental results with the statistical model calculations. Indeed the statistical codes are very well justified for the simulation of neutrons and γ-quanta emission at high-enough excitation energies. However, one has to introduce some additional features to deduce what way the individual levels are ended up in cascades. Sometimes an artificial properties of the cascade are assumed to simplify the calculations. Anyway, the result of statistical calculations is sensitive to the model assumptions and the parameter's choice [16]. The semiempirical analysis could be even more reliable. The important points are certainly to find an appropriate systematizing parameter and to make a selection of the experimental results more or less homogenions by all parameters except the systematizing one.

Let us assume that the product nuclide has only two long-lived states: a low-spin g.s. and a high-spin i.s.. In the statistical model the low probability for the population of an isomeric state is explained by the angular momentum deficit. We therefore try to establish a systematics of the Y_m/Y_g values available by plotting them versus the difference of spin of the input and output channels of the reaction:

$\Delta J = J_t + 1 - J_{i.s.}$,

where J_t and $J_{i.s.}$ are the spins of the initial target nucleus and the produced high-spin isomer, respectively. The dipole radiation spin is taken into account. The reaction yield, which does not end up in the isomeric state, feeds the ground state because of the absence of other long-lived states. The ground state spin therefore does not influence the Y_m/Y_g ratio in such an approximation. Only, when the i.s. and g.s. have nearly equal spins this approach may fail and such cases are excluded from the systematics. A spin-deficit decrease or spin-excess rise allows more probable γ-cascades which lead to a high-spin isomer. So, we can expect the growth of the Y_m/Y_g values as a function of the ΔJ parameter.

The feeding of the final states in reactions proceeds via γ-cascades in the evaporation residue after particle emission. Therefore the levels with excitation energies below the neutron binding energy are involved as initial states for the γ-cascades. The calculated distribution in the E^*, J coordinates for the residual nucleus of the reaction $^{180}Ta^m(\gamma,2n)^{178}Ta$ at E_γ=22 MeV is shown in fig.5. One can see that the wide distribution allows multiple branches of γ-cascades. Fig.5 illustrates that it is not easy to evaluate which cascade will be ended up in the ground state band and which one feeds the special isomeric state.

A distribution type shown in fig.5 could be plotted for the cases of other photonuclear reactions, (γ,n), (γ,p).... In all reactions the peak of distribution is placed near $J_t \pm 1$ by the spin coordinate and closely below B_n by the E^* coordinate. So, one can conclude that all channels of the reactions can be considered together because the distribution preceeding the feeding cascade is more or less unified.

Table 3. Isomeric-to-ground state ratios measured in ref. [17-19] for (γ,n) - reactions.

Reaction	J_t	J_g	J_m	E_e, MeV	Y_m/Y_g	Ref.
$^{142}Nd(\gamma,n)^{141}Nd^{g,m}$	0	3/2	11/2	18	0.04	[17]
$^{144}Sm(\gamma,n)^{143}Sm^{g,m}$	0	3/2	11/2	18	0.036	[17]
$^{153}Eu(\gamma,n)^{152}Eu^{m_1,m_2}$	5/2	0	8	18	0.0075	[18]
$^{185}Re(\gamma,n)^{184}Re^{g,m}$	5/2	3	8	18	0.02	[18]
$^{175}Lu(\gamma,n)^{174}Lu^{g,m}$	7/2	1	6	20	0.10	[19]

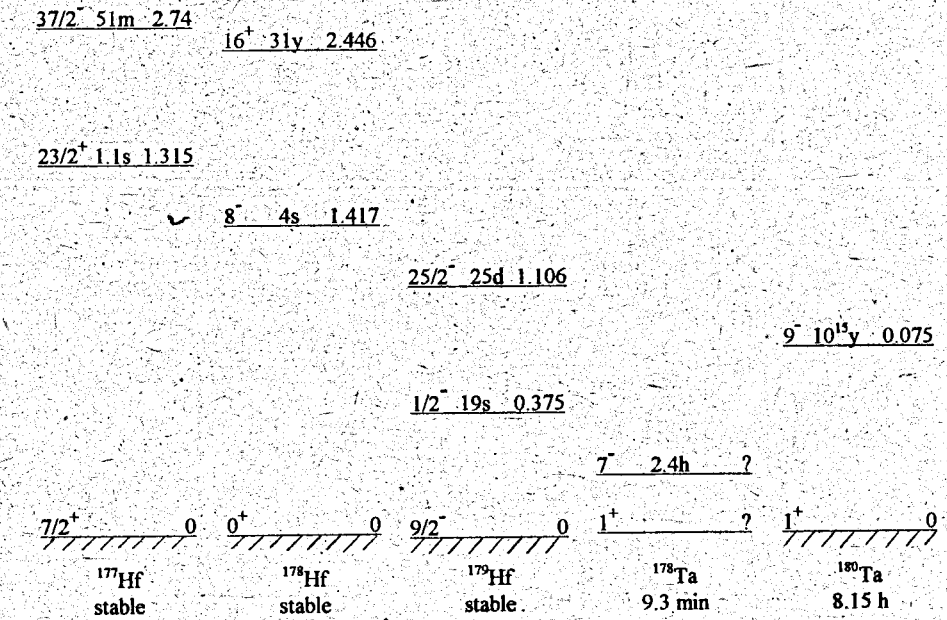

Fig. 1 Isomeric and ground states in Hf and Ta nuclides.

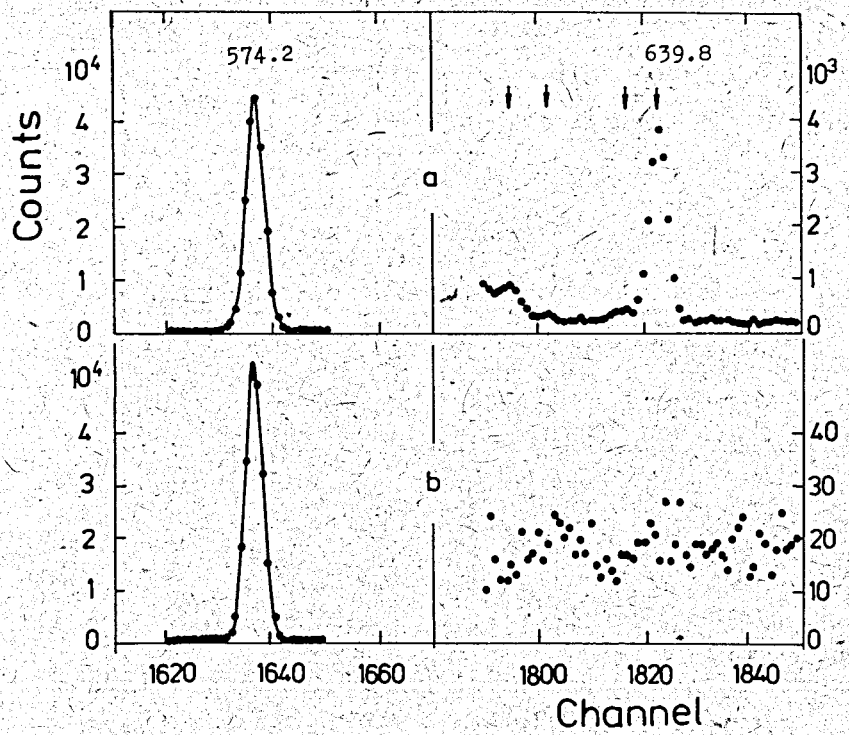

Fig. 2 Portion of the γ-spectra measured for the $^{178}Hf^{m_2}$ source by the Ge detector in close-contact geometry without an absorber (a) and with (7 mm Pb + Cd + Cu) absorber (b).

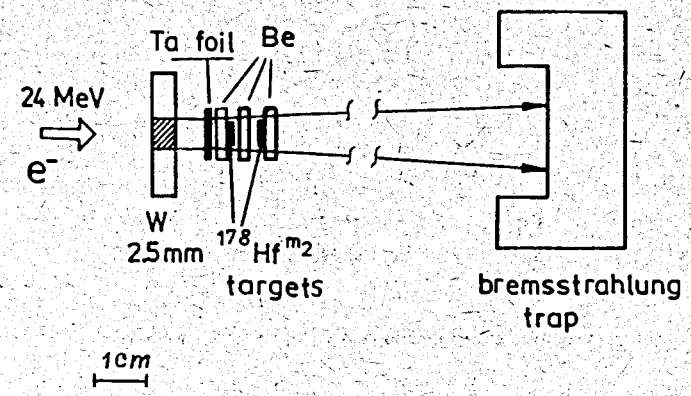

Fig. 3 Schematic layout of the samples activation by the bremsstrahlung from the e-beam of the Dubna MT-25 microtron.

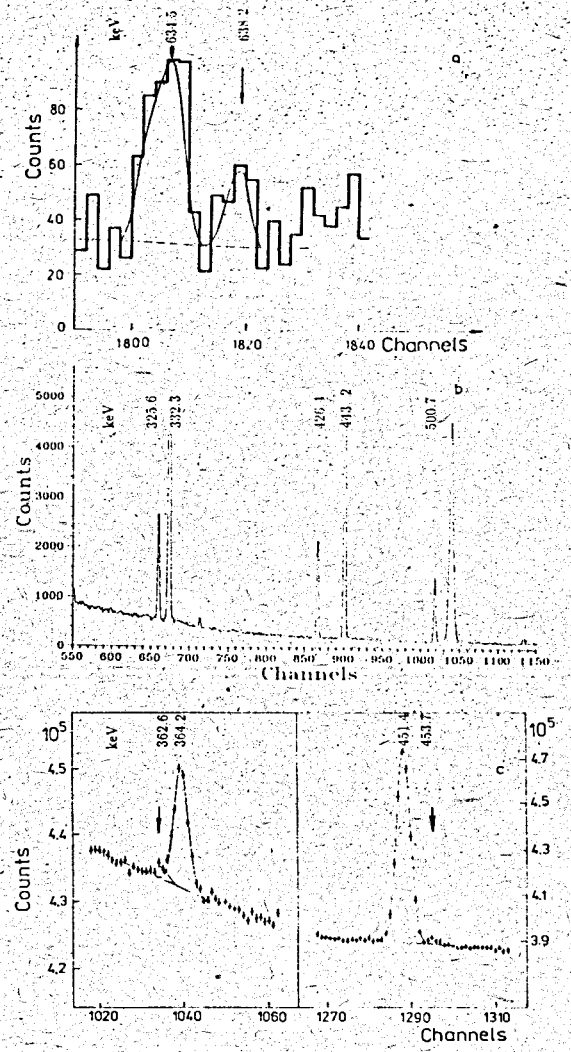

Fig. 4 Fragments of resulting γ-spectra measured for the bremsstrahlung activated isomeric targets:
a) background subtracted spectrum of $^{178}Hf^{m_2}$ (catcher) after activation at $E_e = 23.5$ MeV;
b) spectrum of 10 mg ^{nat}Ta target accumulated during 45 min after 1h cooling (activation at $E_e = 22$ MeV);
c) spectrum of 1 g ^{nat}Ta target accumulated during 110h after 10 day cooling (activation at $E_e = 23.5$ MeV).

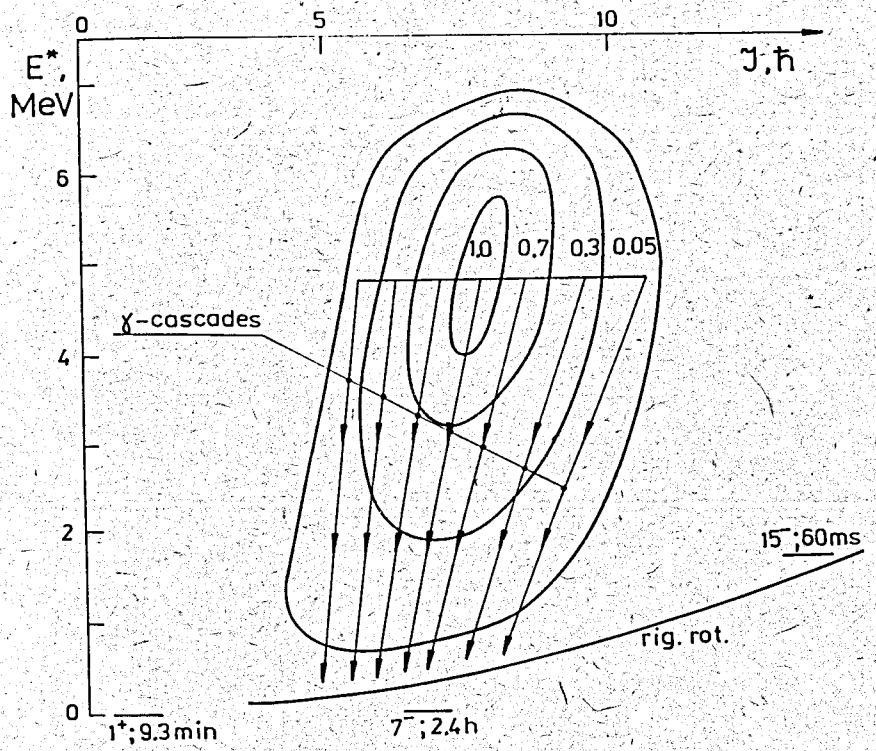

Fig. 5 Contour map of the feeding intensity in the J, E* coordinates for the evaporation residue of the $^{180}Ta^{m}(\gamma, 2n)$ reaction at $E_\gamma = 22$ MeV.

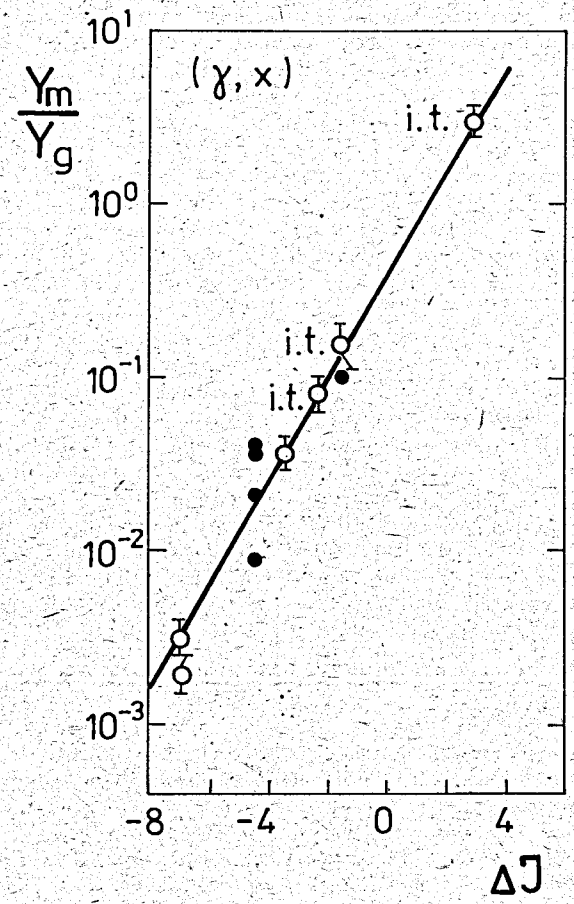

Fig. 6 Isomeric-to-ground state ratios versus spin deficit in photonuclear reactions. Results of the present measurements are shown by opened circles and the literature data [17-19] by full ones. The "i.t." index indicates an isomeric target. The straigt line is a guide by the points.

The reactions on deformed targets from Nd to Re were selected since isomer-to-ground state ratio should be sensitive to a level density parameter. In addition to our results (table 2) we took the literature data [17-19] presented in table 3.

The end-point energy, E_e, of a bremsstrahlung spectrum is another parameter for the data selection. In our measurements the Y_m/Y_g ratios for $^{178}Lu^{m,g}$, $^{180}Hf^{m,g}$ and $^{178}Ta^{m,g}$ were found to be almost independent on E_e in the range of 17-24 MeV. This behaviour does not contradict other experiments and the theory predictions since the J, E^* distribution of excited nuclei is varied slightly when E_e value exceeds the reaction threshold by more than 8 MeV. Finally, we selected the data taken near E_e=20 MeV without any corrections. Not absolutely identical E_e and level density parameters could still bring some irregularities in the data selected.

The systematics is shown in fig.6. One can see that the points are scattered around the straight line demonstrating the exponential growth of the isomeric yields with decreasing spin deficit. For the reaction $^{180}Ta^m(\gamma,2n)^{178}Ta^{m,g}$ where we have an excess of angular momentum (positive ΔJ) the value as high as $Y_m/Y_g = 3$ is reached. This behaviour is understandable in the frame of statistical model approach.

The guide line in fig.6 was drawn by the points corresponding to the low-spin ground state targets. However, one can see that the points for the reactions on high-spin isomeric targets (marked by the index "i.t.") lay on the same line well enough. Thus one can conclude that the selectivity for the population of "target like" single particle states in the photonuclear reaction products, if exists, does not exceed a factor of 1.5. The random scattering of the points does not allow to infer more exactly the selectivity factor. In order to do that one would have to improve the experimental accuracy as well as the theory for the simulation of the Y_m/Y_g values.

5 Conclusion

The isomer-to-ground state ratios have been measured in a group of photon induced reactions on the Hf and Ta targets. Three new photonuclear reactions on high-spin isomeric targets have been observed. The yield values and isomeric-to-ground state ratios have been studied. A systematical behaviour of the isomer-to-ground state ratios versus spin-deficit in the reaction has been demonstrated both for the ground-state and isomeric targets. An additional (to the spin-factor) selectivity for the "target-like" isomeric states population was not revealed. Rather this confirms the presence of total K-mixing at high-excitation energies realized in photonuclear reactions.

Acknowledgements

The authors are grateful to C.B. Collins, J.J. Carroll and Yu.P. Gangrsky for the stimulating discussions. We also want to express our gratitude to the other members of the "Hafnium Collaboration" for their efforts in the production of the $^{178}Hf^{m_2}$ isomer. One of us (S.A.K.) thanks the Ludwig-Maximilians-Universität München for the guest professorship. This work was partially supported by DFG grant Bo 1109/1 and by the Accelerator Laboratory of the Munich Universities, as well as by the collaboration agreement IN2P3-JINR in the frame of the PICS 208.

References

1. Collins, C.B., Eberhard, C.D., Glesener, I.W., Anderson, J.A., Phys. Rev. **C37** 2267 (1988)
2. Collins, C.B., Carroll, J.J. Sinor, T.W., Byrd, M.J., Richmond, D.G., Taylor, K.N., Huber, M., v. Neumann-Cosel, P., Richter, A., Spieler, C., Ziegler, W., Phys. Rev. **C42** 1813 (1990)
3. Schlegel, C., v. Neumann-Cosel, P., Neumeyer, F., Richter, A., Strauch, S., de Boer, J., Dasso, C.H., Peterson, R.T., Phys. Rev. **C50** 2198 (1994)
4. Oganessian, Yu.Ts, Karamian, S.A., Gangrsky, Yu.P., Gorski, B., Markov, B.N., Szeglowski, Z., Briançon, Ch., Le Du, D., Meunier, R., Hussonois, M., Subbotin, M.I., J. Phys. **G18** 393 (1992)
5. Boos, N., Le Blanc, F., Krieg, M., Pinard, J., Huber, G., Lunney, M.D., Le Du, D., Meunier, R., Hussonnois, M., Constantinescu, O., Kim, J.B., Briancon, Ch., Crawford, J.E., Duong, H.T., Gangrski, Y.P., Kühl, T., Markov, B.N., Oganessian, Yu.Ts., Quentin, P., Roussiere, B., Savage, J., Phys. Rev. Lett. **72** 2689 (1994)
6. Rotbard, G., Berrier-Ronsin, G., Constantinescu, O., Fortier, S., Gales, S., Hussonnois, M., Kim, J.B., Maison, J.M., Rosier, L.-H., Vernotte, J., Briancon, Ch., Kulessa, R., Oganessian, Yu.Ts., Karamian, S.A., Phys. Rev. **48** 2148 (1993)
7. Tlusty, P., Venos, D., Kugler, A., Honusek, M., Gorski, B., Phys. Rev. **48** 2082 (1993)
8. Briancon, Ch. for "Hafnium Collaboration", Proc. 8-th Intern. Symp. on Capture Gamma-Ray Spectroscopy (Frieburg) World Scienthific, Singapore (1994)
9. Oganessian, Yu.Ts., Karamian, S.A., Proc. Intern. Conf. on Nucl. Shapes and Nuclear Structure, Antibes, France (1994); and Preprint JINR, E15-94-108, Dubna (1994)
10. Oganessian, Yu.Ts., Karamian, S.A., Gangrski, Yu.P., Gorski, B., Markov, B.N., Szeglowski, Z., Briancon, Ch., Constantinescu, O., Hussonnois, M., Pinard, J., Kulessa, R., Wollersheim, H.J., de Boer, J., Graw, G., Huber, G., Muradian, H.V., Proc. Intern. Symp. Nucl. Phys. of Our Times, p. 521, World Scientific, Singapore (1993)
11. Szeglowski, Z., Dinh Thi Lien, Karamian, S.A., et al., J. Radioanal. Nucl. Chem. Lett. **186 (3)** 233 (1994)
12. Von Lint, V.A., Schmitt, R.A., Suffredini, C.S., Phys. Rev. **121** 1457 (1961)
13. Karamian, S.A., Belov, A.G., Bull. Russian Acad. Sci., Physical issue, **58** 59 (1994)
14. Segebade, Ch., Weize, H.P., Lutz, G., "Photon activation analysis", Berlin, N.Y. (1987)
15. Balabanov, N.P., Belov, A.G., Gangrsky, Yu.P., Kondev, Ph., Tonchev, A., Preprint JINR, E15-93-370, Dubna (1993)
16. Vonach, H.K., Vandenbosch, R., Huizenga, J.R., Nucl. Phys. **60** 70 (1964)

17. Mazur, V.M., Zheltonozhski. V.A., Bigan, Z.M., Russian Journ. Nucl. Phys. **58** 970 (1995)

18. Vishnevski, I.N., Bigan, Z.M., Zheltonozhski, V.A., Mazur, V.M. Nucl. Spectroscopy and Nucl. Structure, Proc. 39-th conf., St.-Petersburg, p.317 (1989); ibid, 38-th conf., p. 323 (1988)

19. Balabanov, N.P., Belov, A.G., Gangrski, Yu.P., Kondev, F.G., Tonchev, A.P., ibid 44-th conf., p. 203 (1994)

Received by Publishing Department
on November 23, 1995.